ISBN: 978-628-95207-8-1. ISSN: 2414-6390. Digital Object Identifier: 10.18687/LACCEI2024.1.1.1887

Road condition monitoring by IRI using sensors implemented on an ATV

Kevin Guerra, BSc.[1], Carlos Raymundo, Ph.D.[1], Manuel Silvera, Msc.[2], and Gianpierre Zapata, Msc.[3]
[1]Research and Development Laboratory in Emerging Technologies, Universidad Peruana de Ciencias Aplicadas, Perú, u201313414@upc.edu.pe, carlos.raymundo@upc.edu.pe
[2] Ingenieria Civil, Universidad Peruana de Ciencias Aplicadas, Perú, manuel.silvera@upc.edu.pe
[3] Escuela Superior de Ingenieria Informatica, Universidad Rey Juan Carlos, Spain, g.zapata.2020@alumnos.urjc.es

***Abstract*– The poor condition of a road causes wear in the mechanics of a vehicle, higher probability of accidents, more traffic and tire wear. To know the conditions of a road it is necessary to monitor the international regularity index (IRI), this calculation is made with different types of manual or automatic recording devices. In Peru, monitoring is done with different types of equipment that, depending on the budget, use different performance and precision systems. At present, manual measurements are still used, which are low cost, but generate errors in the measurement or the process takes too much time and the need to close roads. In this context, the present work aims to automatically monitor the condition of a road through low-cost sensors implemented in an ATV that allows driving in all types of terrain and easily adaptable to ATVs used for patrolling in Peru. Although there are superior advantages in the use of ATVs for the implementation of sensors and automatic monitoring, they present a high level of unwanted vibration due to their size and weight. The system is composed of wavelet transform and moving average filtering techniques for noise reduction and to improve the captured signal for better IRI calculation.**

The results of the system experiments show a monitoring level for each 44 m segment for an average time of 75 seconds, which allows to monitor automatically and in a shorter time large lengths of road.

Keywords—IRI, road, wavelet, accelerometer, ATV.

I. Introduction

Monitoring the condition of a road allows state or private entities to determine the corresponding maintenance or reconstruction actions. The indicator to know the condition of a road is the IRI, this is calculated by means of the differences of a vertical displacement [1]. At present, automatic, and manual systems are used for the collection and calculation of the IRI index. Automatic systems or equipment such as laser profilometers, have as a characteristic a good accuracy in their measurements, but imply a high cost of operation [2].

There are also pivot profilometers that are less expensive to operate but imply the need for a person to handle them, which makes monitoring slow. On the other hand, manual equipment such as Merlin roughness meter tends to generate errors in reading because the acquisition will depend on the experience of the equipment operator. Another manual equipment used for the calculation of the IRI is the topographic level, this instrument allows obtaining accurate data, but it requires at least two people to perform measurements and due to its manual measurement, it demands more time for monitoring [3, 4].

Since the common methods for IRI calculation have a high operating cost, there is a gap for the development of new proposals to minimize the cost and obtain results similar to professional measurement equipment. In [5] and [6], they use integrated sensors of a telephone to collect data, these devices are conditioned to a particular transport vehicle and by means of processing techniques in the frequency domain allow improving the signals and performing the IRI calculation. In works such as [7], [8] and [9], the authors also propose the use of accelerometers integrated in telephones for data capture and the modeling of a quarter car system to obtain suspension parameters to obtain the calculation of the IRI in private transport vehicles. Furthermore, in [8] they perform experiments on the best position of the phone inside a vehicle, performing a calculation with all the accelerometer axes for a global measurement.

In [10] and [11] they propose to calculate the IRI through the sensors of a phone mounted on a bicycle, the data are managed by a mobile application. The experiments are performed on a mountain bike and an urban bike. The authors describe that the collection process requires a balancing effort to acquire good quality data. In [12] and [13], the authors propose to predict the IRI calculation using sensor data collected in previous years, where this information serves as input for a deep learning model to estimate the current year's IRI.

In other works, such as [14] and [15], they collect data using dedicated sensors that are installed in private vehicles, where in [14] the installation is performed inside the vehicle, and they use Kalman filtering methods to predict and correct the vibration signals. In [15], the vibration sensor installation is performed in a seat and the collection is performed with dedicated devices and software for data analysis and processing. On the other hand, in [16], the authors use the Average Root Mean Square Index (ARI) that allows measuring the smoothness of a road. This measure is related to the IRI by means of processing techniques such as Fourier transform, low-pass and high-pass filters, where through tests at different speeds a significant relationship and an improvement of the IRI and ARI indicators is observed after applying the different data processing techniques.

From the state of the art found, it is observed that most of the proposals use sensors integrated in phones, limiting the

Digital Object Identifier: (only for full papers, inserted by LACCEI).
ISSN, ISBN: (to be inserted by LACCEI).
DO NOT REMOVE

sampling rate of the sensors because the phone performs different tasks in the background and the implementation of more sensing points is reduced, due to the low scalability and high cost. Also, it is observed that most of the methods use a private transport vehicle, which depending on the type of vehicle can travel on roads with more or less damage. On the other hand, the use of dedicated sensors and data collection and analysis systems through software increase the operational cost and are limited to the use of hardware with specific characteristics.

In this paper, we propose an automatic IRI calculation system. The system is composed of accelerometers and gyroscopes conditioned on a quadcopter and a data processing algorithm. The use of dedicated sensors allows for small sensing modules, lower cost and higher data sampling rate, collecting more information in less time. These are implemented in an ATV because this type of vehicle can be used in any type of terrain. In addition, due to its reduced size and weight, it allows better maneuverability and displacement.

The paper is structured in three sections, as follows: Sec. II describes the methodology including conditioning, sensor acquisition, data processing and IRI index calculation. In Sec. III, the results of the experiments carried out in two scenarios are presented. Finally, in Sec. IV, we present the main conclusions of the work.

II. Methodology

In the present work, an IRI index monitoring system is proposed that is composed of hardware and software for automatic calculation, as shown in Fig. 1.

A. Data acquisitions

An ATV is used for data acquisition, since this type of vehicle, due to its size, allows greater trafficability on rough and narrow roads. In addition, its use is frequent in different cities of Peru as a surveillance patrol, which allows a quick and lower cost in the deployment of the proposed solution.

The ATV consists of different internal and external structures where electronic monitoring equipment can be adapted. One of the main characteristics of the ATV is its small size and weight, as shown in Table I.

TABLE I
Technical characteristics of the ATV.

Characteristic	Description
Model	Braves 200
Dimensions	1.86 x 1.10 x 1.16 m
Net weight	175 kg
Motor type	OHC Single cylinder 4 strokes
Motor power	12 HP / 7500 RPM
Motor Cylindrical	197 cc

On the other hand, it uses ICM-42688 chips that contain the acceleration and gyroscope sensors, where each one performs measurements in 3 axes (X, Y and Z). The use of this device goes together with a microcontroller ESP32-WROOM, which is responsible for acquiring and packaging the data from the sensors to transmit them via Wi-Fi to the central processor of Raspberry Pi 4B. It is worth mentioning, that the ICM-42688 chip and the ESP32-WROOM microcontroller are housed in a 3D printing structure to perform a better conditioning to the internal structure of the quadcopter. Fig. 2 and 3 show the implementation of each sensor on each side of the ATV.

Data collection is done wirelessly (Wi-Fi) by implementing the MQTT (Message Queuing Telemetry Transport) messaging protocol. This protocol allows data management through publications and subscriptions. Its use allows optimizing response times, battery consumption and bandwidth being focused this protocol for use in the IoT world [17]. For this work, each section of the vehicle where the sensing nodes are hosted, publishes concatenated data from each axis of the gyroscope and accelerometer. Representing each sensing section with the publication name "sensor_left" and "sensor_rigth", as seen in Fig. 4.

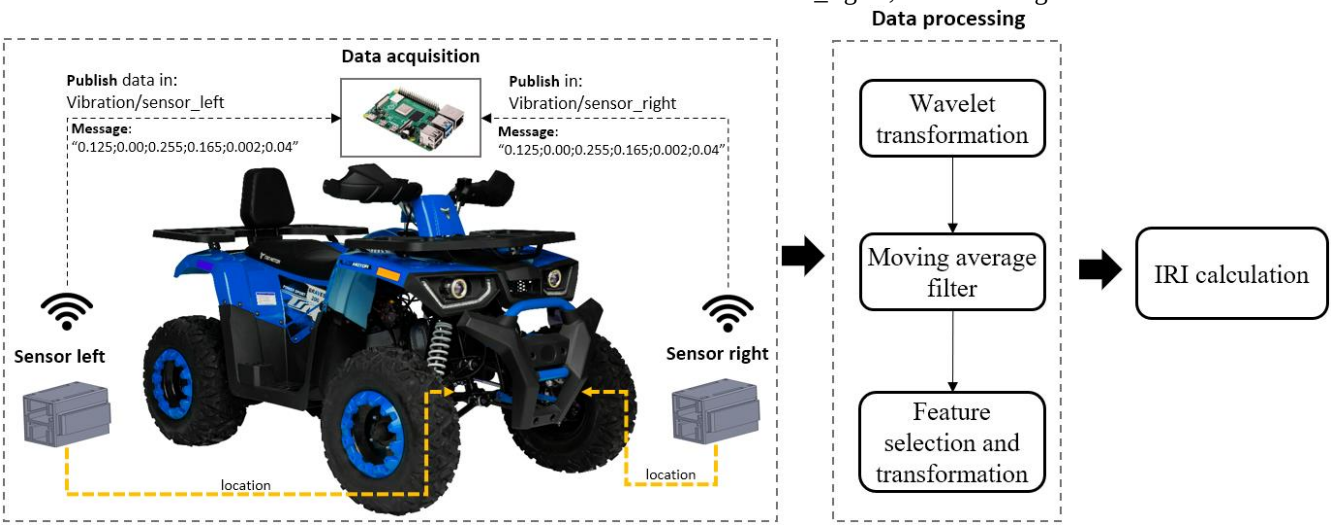

Fig. 1 Diagram of the proposed system.

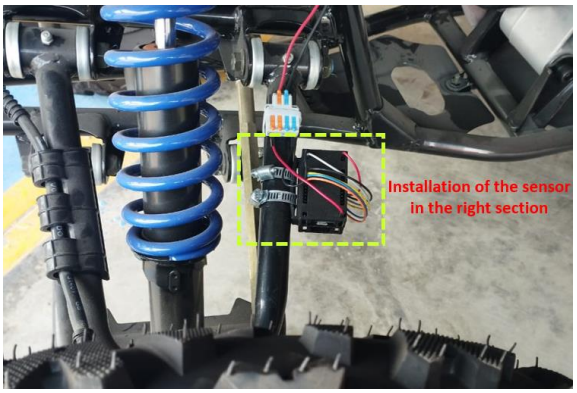

Fig. 2 Right section sensor.

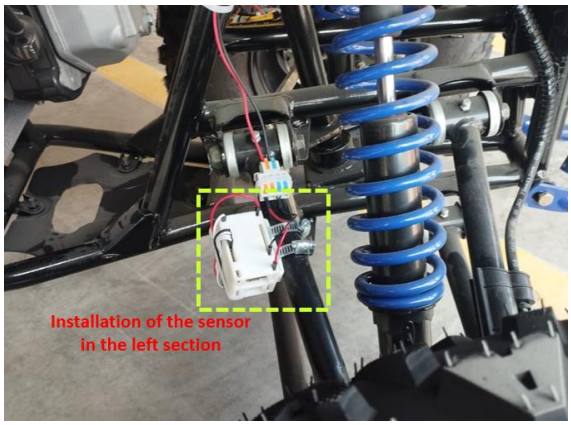

Fig. 3 Left section sensor.

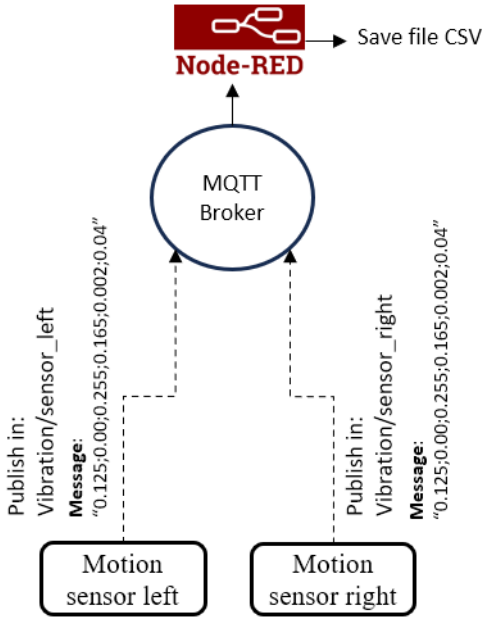

Fig. 4 Data transmission diagram with MQTT protocol.

As part of the implementation of the messaging protocol, a "Brocker" is needed to manage the connections and security settings. Therefore, the Raspberry Pi 4B (central processor) is used as a "Brocker", where through the software tool NodeRed, allows to implement a processing flow scheme that runs and performs an automated process from acquiring data to store them in a CSV file, where each value of each axis is properly aligned. These acceleration and gyroscope data are defined as $a_{t,p}$ and $g_{t,p}$ respectively, where t indicates the axis of each sensor (x, y, z), and p the position of the sensors, left (l) or right (r).

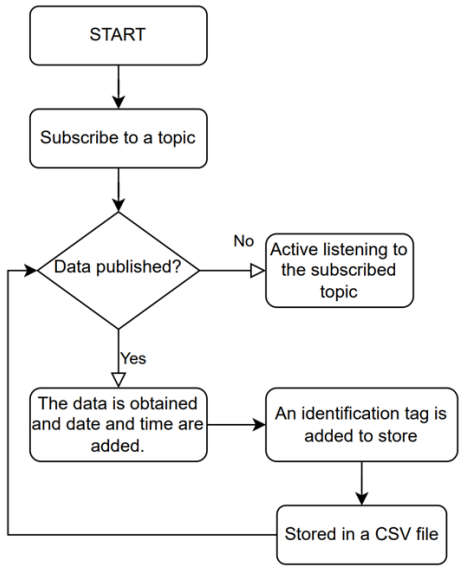

Fig. 5 Flow diagram of the algorithm implemented in Node-RED.

B. *Data processing*

The ATV, being a vehicle with reduced size and weight characteristics, emits vibration noise that is not desired in the algorithm process to be implemented, as shown in Fig. 6. Therefore, a noise reduction process is implemented.

One of the methods implemented for noise reduction is the wavelet transform, which through its subband decomposition of a signal can eliminate or reduce a range of frequencies considered as noise, as described in papers [18] and [19]. For this implementation method, parameters such as decomposition level, type of the wavelet filter and the subbands chosen for reconstruction were taken into account [20]. In this work, a decomposition level 3 and a "Haar" type wavelet filter were used since these parameters allowed observing relevant characteristics of frequency ranges and a lower computational load is used. Then, the subbands chosen for the reconstruction are performed only with the approximation and detail subbands of the last decomposition, since these represent more information and eliminating the high frequencies. Fig. 7 and 8 shows the design of the wavelet decomposition and reconstruction. The result of the wavelet reconstruction is defined as $a_{t,p}^{D}$.

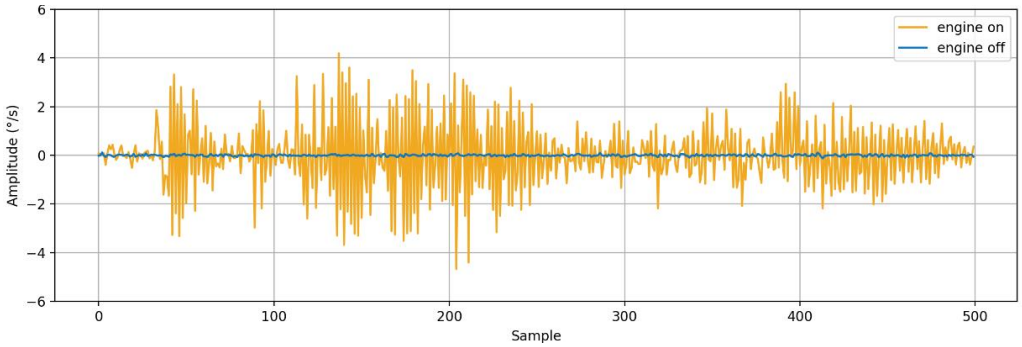

Fig. 6 Vibration generated when the engine is running, and the ATV is parked.

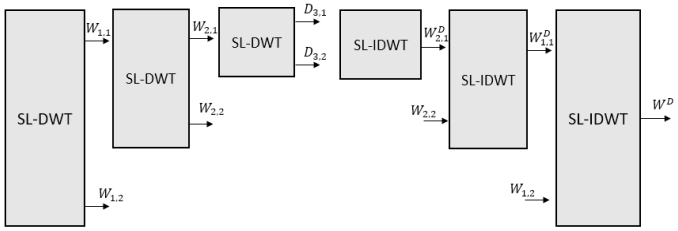

Fig. 7 Wavelet decomposition and reconstruction design

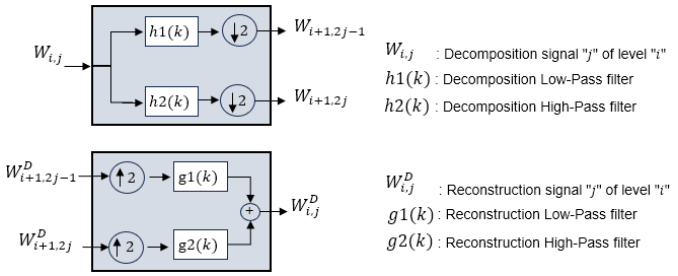

Fig. 8 single-level 1-D discrete wavelet transforms.

From the wavelet reconstruction a noise reduction is observed with peaks of amplitude representing the acquired vibrations from monitoring. However, to further enhance smoothing and reduce high frequencies, the process of moving average filtering is employed. In works such as [21] and [22], better results are obtained for smoothing and noise reduction.

This process is responsible for averaging the amplitudes with respect to a window sample that is sliding over the entire signal [23,24].

As a relevant parameter of moving average filtering is the window size, expressed in the Eq. 1. For this work a size of M = 5 samples was set, since a larger size would perform a more pronounced filtering abruptly decreasing the signal amplitudes and losing information of amplitude peaks that represent the collected vibrations. Fig. 9 shows the result of the noise reduction by applying the two processing methods mentioned above.

$$A_{t,p}[i] = \frac{1}{M}\sum_{j=0}^{M-1} a^{D}_{t,p}[i+j] \quad (1)$$

C. *IRI calculating*

The IRI measurement shows the condition of a road by means of the vertical variations that are acquired by sensors, this allows to know the roughness of a road, relating the resulting values to a certain state or condition of breathability. In this work, the interpretation of the results was used taking into account the regulations detailed in [25], since they are specific for Peruvian territory. Table II shows the relationship between IRI values and the condition of a road.

In related works, the calculation of the IRI is performed by simplifying the quarter-car model.

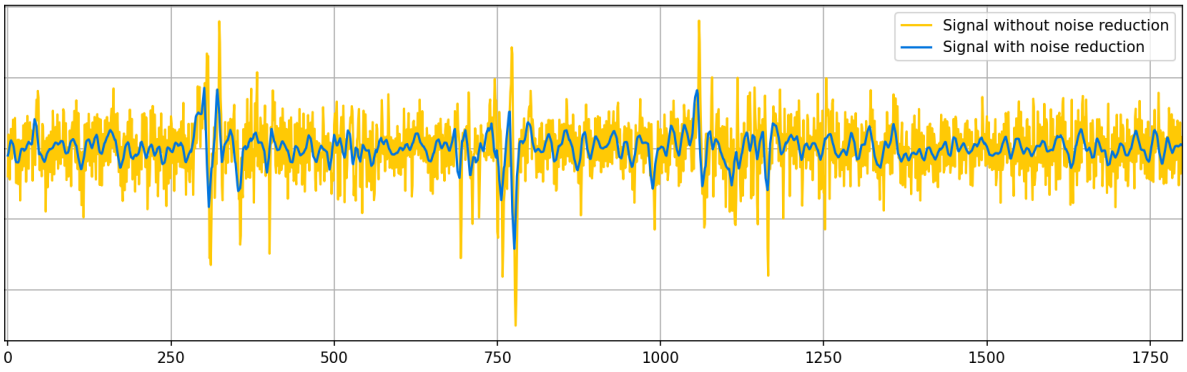

Fig. 9 result of applying noise reduction techniques.

TABLE II
IRI classification.

Classification	IRI Ranges
Very Good	0 – 1.4
Good	1.4 – 2.3
Fair	2.3 – 3.6
Poor	3.6 – 6.0
Very low	> 6.0

Therefore, taking the calculation process of [10] and [26], Eq. 2 is obtained, where t_{start} is the capture start time, t_{end} is the capture finished time, ts is the monitored road distance and av is the vertical acceleration that provides information of the acceleration amplitude changes in the z-axis. In [10] they mention that due to the position of the implementation of the sensors in the vehicles a deflection or tilt can be introduced that can decrease the information of the signals in the vertical z-axis. Therefore, the use of Eq. 3 is proposed, where the vertical acceleration is calculated by the magnitude of the signals from the three axes and the average of the signals from the three axes for 5 seconds, which serves as a more stable measure. Obtaining the most accurate vertical acceleration variable.

$$IRI_p = \frac{\iint_{t_{start}}^{t_{end}} |av_p| \, (dt)^2}{tr} \tag{2}$$

$$av_p = \frac{A_p . \overline{A_p}}{|\overline{A_p}|} = A_{x,p} * \overline{A_{x,p}} + A_{y,p} * \overline{A_{y,p}} + A_{z,p} * \overline{A_{z,p}} \tag{3}$$

Where

p: indicates the position of the sensor.
A_p: accelerations capture.
$\overline{A_p}$: average of each acceleration axis.
av_p: vertical acceleration.

In this work, by using sensors in each section of the quadricycle (right and left), two IRI measurements are obtained, therefore, the final IRI calculation is made by averaging the IRI of the two monitored sections, as shown in the following equation.

$$IRI_m = \frac{IRI_l + IRI_r}{2} \tag{4}$$

Where

IRI_m: Average IRI.
IRI_r: IRI calculation right side.
IRI_l: IRI calculation left side.

D. Scenario

The scenario used for the experiment is carried out in the city of Santiago de Surco located in Lima-Peru. This scenario consists of a flexible pavement road where the monitoring distance is 4 km having a start and end at coordinates (-12.108350, -76.963719) and end (-12.103662, -76.956822), respectively. For the scenario, measurements are made in segments of 44 meters, which results in 47 segments where the IRI is obtained. In addition, the speed of the ATV is set at 10 km /h on average. Fig. 10 shows the experiment scenario from a top map view.

II. Results

The experiment performed in the scenario described in previous sections shows IRI values that are related to the number of failures found in the scenario. Where the obtained IRI values indicate that the classification varies between "very good", "good" and "fair". These classifications help audit institutions to make decisions in an optimal way.

In addition, the process from data capture to data processing for the approximately 2 km of the route was 26 min. This indicates the speed of monitoring the condition of a road and the automation of the proposed system. Fig. 11 and 12 show the results by 44 m segments for a breakdown and further analysis information.

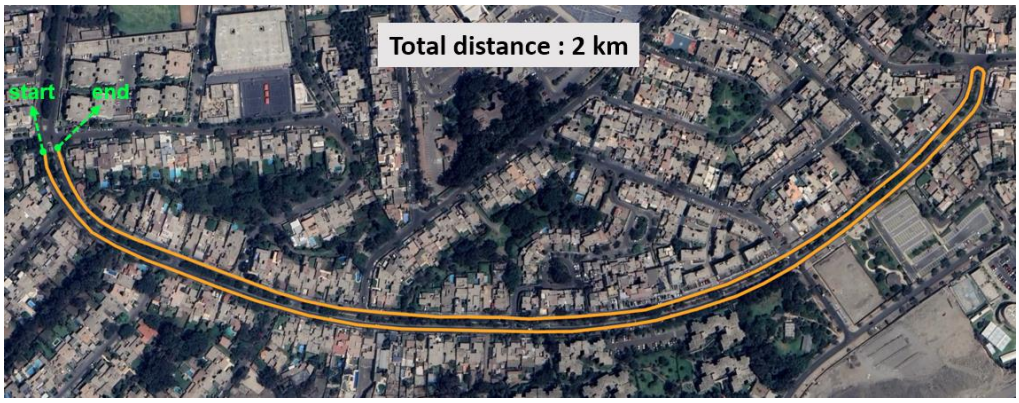

Fig. 10 Trajectory of the monitored experiment.

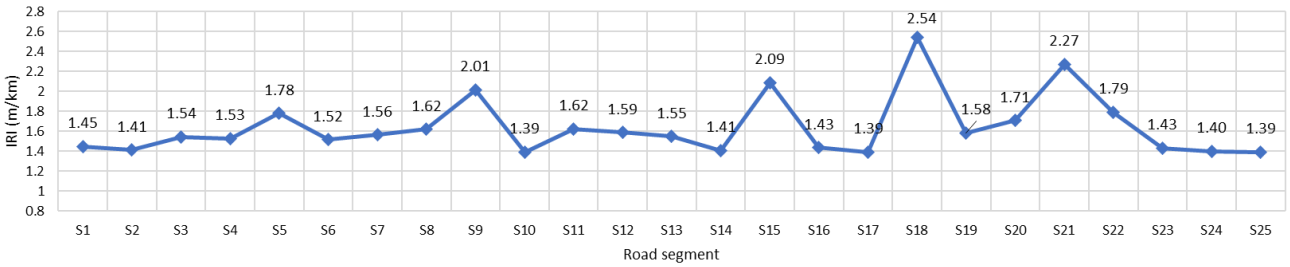

Fig. 11 IRI monitored in 25 segments.

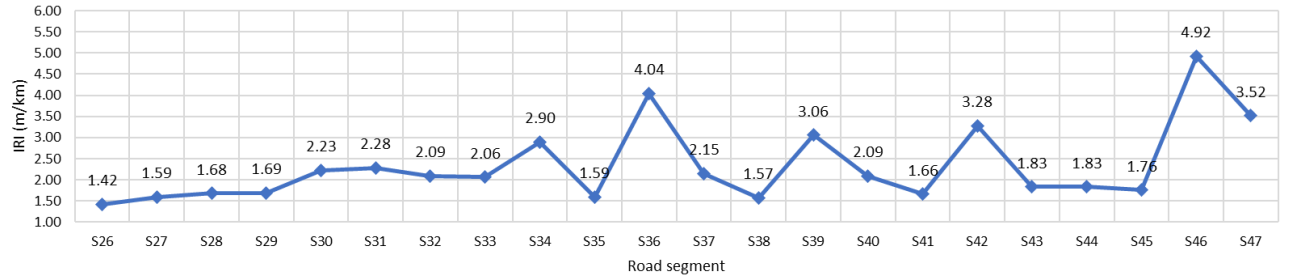

Fig. 12 IRI monitored in 22 remaining segments.

IV. Conclusion

In this paper, we have introduced a proposed system based on monitoring the condition of a road through the calculation of the IRI, where the sensors are implemented in an ATV that allows a low-cost solution, transit on any type of road and continuous use through implementation in patrolling ATVs for public safety.

The results of the experiments show that the proposed system performs monitoring every 44 m in an average time of 75 seconds. In addition, the use of sensors not integrated in phones allows maximizing the performance of the sensors and greater scalability in monitoring multiple points.

The proposed system conditioned on patrolling ATVs would improve the continuous monitoring of the condition of a road, which benefits in decision making both in budgeting, maintenance, etc.

In our implementation, we consider low complexity signal processing algorithms or techniques to optimize power consumption and hardware requirement. In the future, we intend to integrate cloud link functionalities and an adaptation of distance and speed sensors to combine information and obtain data with better accuracy.

References

[1] D. S. Eric J. Zamora Alvarez John B. Ferris and E. Horn, 'Development of a discrete roughness index for longitudinal road profiles', International Journal of Pavement Engineering, vol. 19, no. 12, pp. 1043–1052, 2018.

[2] N. Abulizi, A. Kawamura, K. Tomiyama, and S. Fujita, 'Measuring and evaluating of road roughness conditions with a compact road profiler and ArcGIS', Journal of Traffic and Transportation Engineering (English Edition), vol. 3, no. 5, pp. 398–411, 2016.

[3] P. Johannesson, K. Podgórski, and I. Rychlik, 'Laplace distribution models for road topography and roughness', International Journal of Vehicle Performance, vol. 3, no. 3, pp. 224–258, 2017.

[4] Y. Qiao, S. Chen, M. Alinizzi, M. Alamaniotis, and S. Labi, 'Estimating IRI based on pavement distress type, density, and severity: Insights from machine learning techniques', arXiv [stat.AP]. 2021.

[5] A. Montha, A. Huytook, T. Rakmark, and P. Lertworawanich, 'Road Roughness Estimation Using Acceleration Data from Smartphones', in Advances in Road Infrastructure and Mobility, 2022, pp. 407–415.

[6] V. S. L. Janani and S. Mathew, 'Influence of surface distresses on smartphone-based pavement roughness evaluation', International Journal of Pavement Engineering, vol. 22, no. 13, pp. 1637–1650, 2021.

[7] S. X. Zhen Zhang Hongliang Zhang and W. Lv, 'Pavement roughness evaluation method based on the theoretical relationship between acceleration measured by smartphone and IRI', International Journal of Pavement Engineering, vol. 23, no. 9, pp. 3082–3098, 2022.

[8] J. Zeng, J. Zhang, Q. Cao, and W. Guo, 'Research on Vibration Index of IRI Detection Based on Smart Phone', in Proceeding of 2021 International Conference on Wireless Communications, Networking and Applications, 2022, pp. 1067–1076.

[9] K. R. Opara, K. Brzeziński, M. Bukowicki and K. Kaczmarek-Majer, "Road Roughness Estimation Through Smartphone-Measured Acceleration," in IEEE Intelligent Transportation Systems Magazine, vol. 14, no. 2, pp. 209-220, March-April 2022, doi: 10.1109/MITS.2021.3049382

[10] K. Zang, J. Shen, H. Huang, M. Wan, and J. Shi, 'Assessing and Mapping of Road Surface Roughness based on GPS and Accelerometer Sensors on Bicycle-Mounted Smartphones', Sensors, vol. 18, no. 3, 2018.

[11] A. Aboah, M. Boeding, and Y. Adu-Gyamfi, 'Mobile Sensing for Multipurpose Applications in Transportation', Journal of Big Data Analytics in Transportation, vol. 4, no. 2, pp. 171–183, Dec. 2022.

[12] A. Aboah and Y. Adu-Gyamfi, 'Smartphone-Based Pavement Roughness Estimation Using Deep Learning with Entity Embedding', Advances in Data Science and Adaptive Analysis, vol. 12, no. 03n04, p. 2050007, 2020.

[13] E. E. Ekpenyong, A. S. P. Abu and K.Z. Cinfwat, 'Comparative Study of the Road Roughness Measurement of Roadlab Pro and Roadroid Applicatons for IRI Data Collection in Nigeria', The International Journal of Engineering and Science, vol. 10, no. 05, pp. 14–19, May 2021.

[14] J. Li, L. Wang, Y. Miao, X. Tong, and Z. Ye, 'Road Roughness Detection Based on Discrete Kalman Filter Model with Driving Vibration Data

Input', International Journal of Pavement Research and Technology, Aug. 2023.
[15]J. Zhang, L. Wang, P. Jing, Y. Wu, and H. Li, 'IRI Threshold Values Based on Riding Comfort', Journal of Transportation Engineering, Part B: Pavements, vol. 146, no. 1, p. 04020001, 2020.
[16]C.-P. Chou, G.-J. Siao, A.-C. Chen, and C.-C. Lee, 'Algorithm for Estimating International Roughness Index by Response-Based Measuring Device', Journal of Transportation Engineering, Part B: Pavements, vol. 146, no. 3, p. 04020031, 2020.
[17]M. B. Yassein, M. Q. Shatnawi, S. Aljwarneh, and R. Al-Hatmi, 'Internet of Things: Survey and open issues of MQTT protocol', in 2017 International Conference on Engineering & MIS (ICEMIS), 2017, pp. 1–6.
[18]M. F. Pouyani, M. Vali, and M. A. Ghasemi, 'Lung sound signal denoising using discrete wavelet transform and artificial neural network', Biomedical Signal Processing and Control, vol. 72, p. 103329, Feb. 2022.
[19]G. Baldazzi et al., 'Systematic analysis of wavelet denoising methods for neural signal processing', Journal of Neural Engineering, vol. 17, no. 6, p. 066016, Dec. 2020.
[20]K. Guerra, J. Casavilca, S. Huamán, L. López, A. Sanchez, and G. Kemper, 'A low-rate encoder for image transmission using LoRa communication modules', International Journal of Information Technology, vol. 15, no. 2, pp. 1069–1079, Feb. 2023.
[21]D. Zhang et al., 'An ECG Signal De-Noising Approach Based on Wavelet Energy and Sub-Band Smoothing Filter', Applied Sciences, vol. 9, no. 22, 2019.
[22]F. Crenna, G. B. Rossi, and M. Berardengo, 'Filtering Biomechanical Signals in Movement Analysis', Sensors, vol. 21, no. 13, 2021.
[23]D. T. Thinh, N. B. H. Quan, and N. Maneetien, 'Implementation of Moving Average Filter on STM32F4 for Vibration Sensor Application', in 2018 4th International Conference on Green Technology and Sustainable Development (GTSD), 2018, pp. 627–631.
[24]G. Kemper, A. Oshita, R. Parra, and C. Herrera, 'An algorithm for obtaining the frequency and the times of respiratory phases from nasal and oral acoustic signals', International Journal of Electrical and Computer Engineering, vol. 13, no. 1, pp. 358–373, 2023.
[25]L. H. Tingal, "Análisis del Índice de Rugosidad Internacional de la superficie del pavimento flexible de la vía Cajamarca-Baños del Inca, utilizando el rugosímetro de Merlín," B.Sc. tesis, Universidad Nacional de Cajamarca, Cajamarca, Perú, 2021.
[26]W. Aleadelat, K. Ksaibati, C. H. G. Wright, and P. Saha, 'Evaluation of Pavement Roughness Using an Android-Based Smartphone', Journal of Transportation Engineering, Part B: Pavements, vol. 144, no. 3, p. 04018033, 2018.